

Constraints on the gas masses of low- z damped Lyman- α systems

Parichay Mazumdar^{1,2}, Nissim Kanekar^{2*} and J. Xavier Prochaska³

¹*St. Stephen's College, University Enclave, New Delhi 110007, India*

²*National Centre for Radio Astrophysics, Tata Institute of Fundamental Research, Ganeshkhind, Pune 411007, India*

³*UCO/Lick Observatory, UC Santa Cruz, Santa Cruz, CA 95064, USA*

Accepted yyyy month dd. Received yyyy month dd; in original form yyyy month dd

ABSTRACT

We report a deep search for redshifted H α 21cm emission from three damped and sub-damped Lyman- α absorbers (DLAs) at $z \approx 0.1$ with the Green Bank Telescope (GBT). No evidence for a redshifted H α 21cm emission signal was obtained in the GBT spectra of two absorbers, with the data on the third rendered unusable by terrestrial interference. The non-detections of H α 21cm emission yield strong constraints on the H α masses of the associated galaxies, $M_{\text{HI}} < 2.3 \times 10^9 \times (\Delta V/100)^{1/2} M_{\odot}$ for the sub-DLA at $z = 0.0830$ towards J1553+3548, and $M_{\text{HI}} < 2.7 \times 10^9 \times (\Delta V/100)^{1/2} M_{\odot}$ for the DLA at $z = 0.0963$ towards J1619+3342, where ΔV is the H α 21cm line width, in km s $^{-1}$. This continues the trend of low H α masses found in all low- z DLAs and sub-DLAs that have been searched for redshifted H α 21cm emission. Low-redshift absorbers with relatively low H α column densities, $\lesssim \text{few} \times 10^{20} \text{ cm}^{-2}$, thus do not typically arise in massive gas-rich galaxies.

Key words: galaxies: evolution: – galaxies: high redshift – quasars: absorption lines – radio lines: galaxies

1 INTRODUCTION

Understanding the nature of the galaxies that give rise to damped Lyman- α systems (DLAs) and their redshift evolution has been an important question in galaxy evolution for nearly thirty years. With H α column densities $\geq 2 \times 10^{20} \text{ cm}^{-2}$, similar to those seen on sightlines through local galactic disks, DLAs are the highest H α column density systems detected in absorption in the optical and ultraviolet (UV) spectra of background quasars and are presumably the high- z counterparts of today's normal galaxies. Further, while the H α content of high- z DLAs is insufficient (by about a factor of 2) to entirely fuel the stars observed in today's galaxies (e.g. Prochaska et al. 2005; Noterdaeme et al. 2009), DLAs contain the bulk of the neutral hydrogen at high redshifts ($\approx 80\%$; e.g. O'Meara et al. 2007).

The fact that DLAs are selected to lie along the sightline to bright quasars implies that it is difficult to directly image the host galaxies, and estimate their stellar masses and star formation rates (SFRs). Indeed, despite numerous searches, galaxy counterparts have been identified and/or SFRs estimated for only about ten DLAs at $z \geq 2$ (see, e.g., Krogager et al. 2012, and references therein), with a few more systems identified at $z \approx 1$ (e.g. Péroux et al. 2012). It is also clear from these studies that typical high- z DLAs have low SFRs, $\lesssim 1 - 10 M_{\odot} \text{ yr}^{-1}$, making them additionally difficult to detect in optical/near-infrared line or continuum emission (e.g. Fumagalli et al. 2010). Finally, sensitivity issues with current radio telescopes have precluded the detection of,

or even useful limits on, radio H α 21cm or CO line emission from high- z DLAs (e.g. Wiklind & Combes 1994; Kanekar et al. 2006).

Most of our information on DLAs at all redshifts hence stems from absorption spectroscopy. For example, optical and UV spectroscopy have yielded estimates of metallicities and abundances in a large number of DLAs out to $z \sim 5$ (see Rafelski et al. 2012, and references therein). DLA metallicities are now known to evolve with redshift, with the average metallicity higher at low redshifts (e.g. Prochaska et al. 2003; Rafelski et al. 2012); however, low metallicities are typical at all redshifts. The correlations observed between DLA metallicities and both the velocity widths or rest equivalent widths of low-ionization metal lines (Wolfe & Prochaska 1998; Ledoux et al. 2006; Prochaska et al. 2008) suggest the presence of a mass-metallicity relation in DLAs (e.g. Møller et al. 2013; Neeleman et al. 2013), as has been observed in other high- z galaxies (e.g. Tremonti et al. 2004). High- z DLAs have been shown to have low molecular fractions, typically $\lesssim 10^{-5}$, with only one-sixth showing detectable H $_2$ absorption (e.g. Ledoux et al. 2003; Noterdaeme et al. 2008). High- z DLAs also have low fractions of cold atomic gas, with most of the H α in the warm phase for absorbers at $z \geq 2$ (e.g. Kanekar & Chengalur 2003; Kanekar et al. 2014), apparently due to the low DLA metallicities and hence, the paucity of cooling routes (Kanekar & Chengalur 2001; Kanekar et al. 2009). Low-ionization metal lines detected in DLAs tend to have multiple components, sometimes with very different relative abundances (e.g. Dessauges-Zavadsky et al. 2006; Kanekar et al. 2006), and large velocity widths, $\gtrsim 90 \text{ km s}^{-1}$ (Prochaska & Wolfe 1997).

While the above results provide insight on physical conditions

* E-mail: nkanekar@ncra.tifr.res.in

in DLAs, they only trace conditions along the narrow pencil beam towards the background QSO. There is hence often ambiguity in their interpretation, even in terms of the big-picture view (e.g. large disk galaxies versus small merging systems; Prochaska & Wolfe 1997; Haehnelt et al. 1998). As a result, we as yet have very little information on the basic physical characteristics of high- z DLAs, especially their mass and size.

At low redshifts, Hubble Space Telescope and ground-based imaging of DLA fields have found DLAs to arise in a range of galaxy types, from dwarfs to large spiral disks (e.g. le Brun et al. 1997; Rao et al. 2003; Chen et al. 2005), consistent with the general galaxy population (e.g. Zwaan et al. 2005). However, these results have been limited both by the small sample size and by concerns that a fainter galaxy at yet smaller impact parameter (i.e. beneath the quasar) might be responsible for the DLA absorption. As such, the crucial missing pieces in our understanding of DLA evolution remain the masses and sizes of the absorbing galaxies.

Low- z DLAs offer the exciting possibility of resolving the above issues through a direct measurement of the H I mass, the spatial extent of the neutral gas and the gas velocity field, via H I 21cm emission observations. Unlike optical imaging studies, which, even for low- z DLAs are typically stymied by the quasar (although see Fumagalli et al. 2010), H I 21cm observations permit detections of galaxies at all impact parameters from the quasar sightline. And, of course, it would be possible to relate the measured properties to the characteristics of the DLA obtained from optical/UV absorption spectroscopy (e.g. metallicities, abundances, etc) and optical/UV imaging (e.g. star formation rates, stellar masses, etc) to obtain a comprehensive picture of the absorbing galaxies.

Until recently, the weakness of the H I 21cm transition as well as the lack of damped and sub-damped Lyman- α absorbers at low redshifts, $z \lesssim 0.2$ had limited searches for H I 21cm emission to three absorbers, at $z = 0.0063$ towards PG 1216+069 (Kanekar & Chengalur 2005; Briggs & Barnes 2006), at $z = 0.009$ towards SBS1549+543 (Bowen et al. 2001; Chengalur & Kanekar 2002) and $z = 0.101$ towards PKS 0439–433 (Kanekar et al. 2001). The high far-ultraviolet sensitivity of the new *Cosmic Origins Spectrograph* (COS) onboard the *Hubble Space Telescope* (HST) has resulted in the detection of three new DLAs and sub-DLAs at $z \approx 0.1$ (Meiring et al. 2011). In this *Letter*, we report a search for redshifted H I 21cm emission from these absorbers, at $z = 0.0830$ towards J1553+3548, $z = 0.0963$ towards J1619+3342 and $z = 0.1140$ towards J1009+0713, using the Green Bank Telescope (GBT).

2 OBSERVATIONS, DATA ANALYSIS AND RESULTS

The GBT L-band receiver was used for the observations between June and September 2011, with the AutoCorrelation Spectrometer (ACS) as the backend, four 50 MHz ACS sub-bands, two linear polarizations, and 10-second records. The same frequency settings were used for all four absorbers, with three ACS sub-bands centred on the three redshifted H I 21cm line frequencies, so as to test for radio frequency interference (RFI). Each ACS sub-band was divided into 8192 spectral channels, yielding a velocity resolution of $\approx 1.4 \text{ km s}^{-1}$ and a total velocity coverage of $\approx 11,500 \text{ km s}^{-1}$ for each absorber. Position switching was used to calibrate the passband shape, with a 10-min. On/Off cycle, while the flux density scale was determined via online system temperature measurements with a blinking noise diode. The total observing time was 9 hours (J1553+3548), 11 hours (J1619+3342) and 33 hours

(J1009+0713). Note that more time was spent on the $z = 0.1140$ DLA towards J1009+0713 as strong RFI was detected during the observations at $\approx 1275 \text{ MHz}$, close to its redshifted H I 21cm line frequency.

All data were analysed using DISH, the AIPS++ single-dish package. Detailed data editing was necessary, due to the presence of significant amounts of RFI in all datasets as well as ACS failures. This was done via visual inspection of the calibrated dynamic spectra. About 20% of the data had to be edited out for the absorbers towards J1553+3548 and J1619+3342, while the data towards J1009+0713 were entirely unusable. After the data editing, the individual spectra were calibrated, with a second-order baseline fit to each 10-second spectrum and subtracted out. The Hanning-smoothed and re-sampled spectra were then averaged together, to produce a spectrum for each observing epoch. For each source, the spectra from different epochs were shifted to the barycentric frame and then averaged together, using weights based on the root-mean-square (RMS) noise values. The final spectra for the absorbers towards J1553+3548 and J1619+3342 had RMS noise values of $\approx 0.65 \text{ mJy}$ per 2.8 km s^{-1} channel; these are shown in the two top panels of Fig. 1.

The search for redshifted H I 21cm emission was carried out after smoothing the spectra to, and re-sampling at, velocity resolutions of $\approx 20, 40$, and 100 km s^{-1} . The lower panels of Fig. 1 show the two H I 21cm spectra at velocity resolution of $\approx 100 \text{ km s}^{-1}$. The grey shaded regions indicate frequency ranges affected by narrow-band RFI, while the dashed vertical line marks the expected redshifted H I 21cm line frequency. It is clear that there is no evidence for either RFI or H I 21cm line emission within $\approx 350 \text{ km s}^{-1}$ of the expected redshifted line frequencies. The RMS noise values at a velocity resolution of $\approx 100 \text{ km s}^{-1}$ are 0.22 mJy (J1553+3548) and 0.19 mJy (J1619+3342).

3 DISCUSSION

The three DLAs and sub-DLAs that were observed with the GBT were discovered via *HST-COS* ultraviolet spectroscopy of a set of background quasars, selected for studies of gas at entirely different redshifts (Meiring et al. 2011; Tumlinson et al. 2013). The absorber redshifts are well-constrained by both the Ly α and associated metal-line transitions to an accuracy better than a few tens of km s^{-1} (Battisti et al. 2012). The metal-line transitions also enable estimates of the gas-phase elemental abundances, and hence, the absorber metallicities. The three absorbers studied here have metallicities (relative to solar) of $[Z/H] = -1.12$ to -0.54 , using S or Si abundances, and making appropriate ionization corrections for the sub-DLA towards J1553+3548 (Battisti et al. 2012).

Our GBT non-detections of H I 21cm line emission can be used to place constraints on the total H I mass of the two absorbers, using the relation (e.g. Rohlfs & Wilson 2006)

$$M_{\text{HI}} = 2.356 \times 10^5 \times D_L^2 \times (1+z)^{-1} \times \int S dV, \quad (1)$$

where M_{HI} (in M_\odot) is the H I mass of the galaxy, z is its redshift, D_L (in Mpc) is its luminosity distance¹, and $\int S dV$ (in Jy km s^{-1}) is the velocity integral of the H I 21cm line flux density.

For non-detections of H I 21cm emission, one must assume a

¹ We use a Λ -Cold Dark Matter (Λ CDM) cosmology, with $H_0 = 67.3 \text{ km s}^{-1} \text{ Mpc}^{-1}$, $\Omega_m = 0.315$ and $\Omega_\Lambda = 0.685$ (Planck Collaboration 2013).

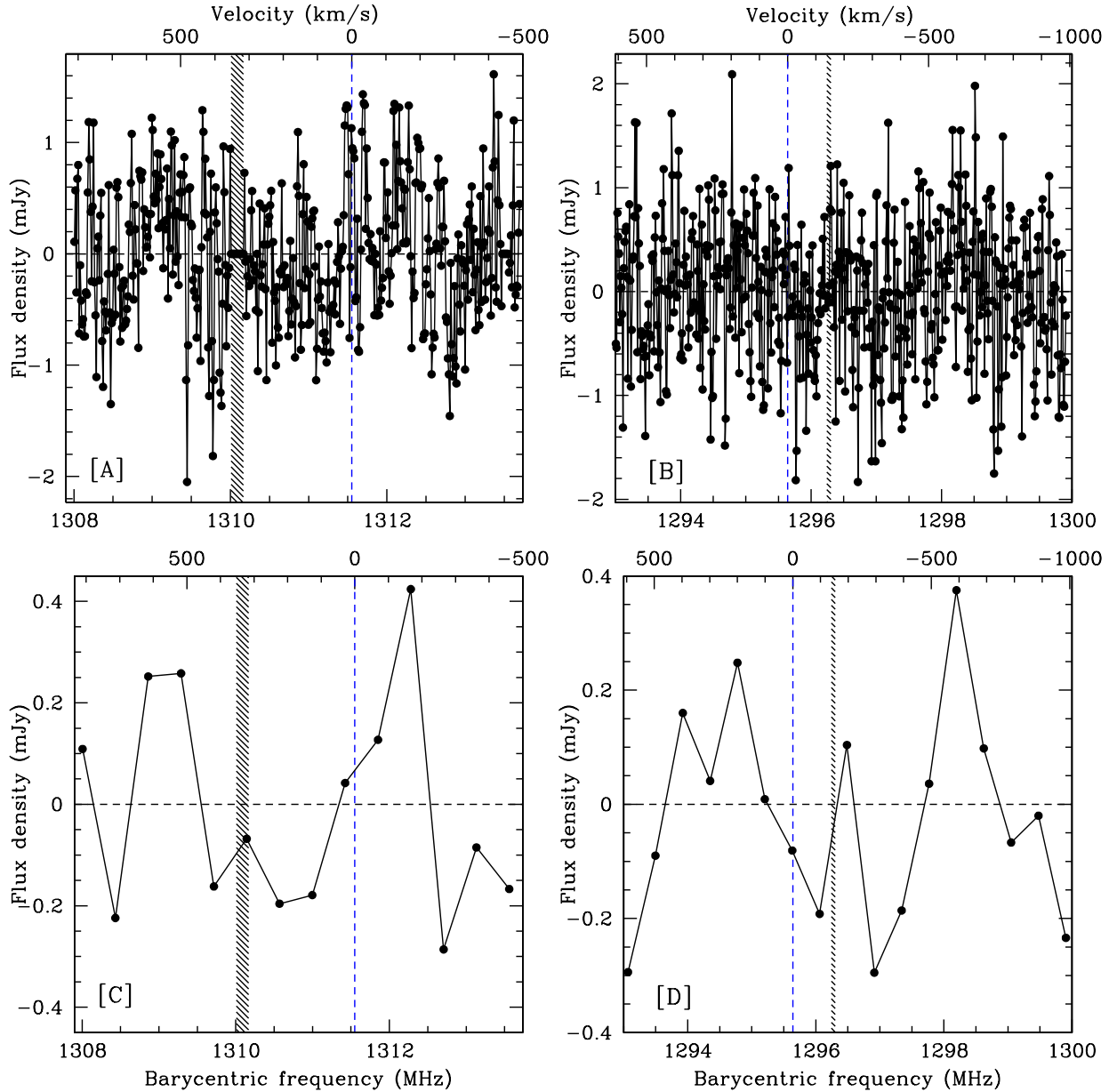


Figure 1. GBT H I 21cm spectra from the $z = 0.0830$ sub-DLA towards J1553+3548 (left panels) and the $z = 0.0963$ DLA towards J1619+3342 (right panels). The x-axis of each panel is barycentric frequency (in MHz), the y-axis is flux density (in mJy), while the top axis shows velocity (in km s^{-1}), relative to the absorber redshift. The top panels ([A] and [B]) show the spectra at a velocity resolution of 2.8 km s^{-1} , after Hanning-smoothing and re-sampling; the lower two panels ([C] and [D]) show the spectra after smoothing to a velocity resolution of $\approx 100 \text{ km s}^{-1}$. The shaded regions indicate frequency ranges affected by RFI, while the dashed vertical line marks the expected location of the H I 21cm emission line.

velocity distribution for the emitting gas to derive limits on the H I mass. Note that, for a given H I mass, a galaxy with a narrower H I 21cm emission profile would yield a lower peak line flux density. We will assume the H I 21cm emission profiles to be Gaussian, with a line full-width-at-half-maximum $\Delta V = 100 \text{ km s}^{-1}$. This yields 3σ upper limits of $\int S dV < 0.060 \times (\Delta V/100)^{1/2} \text{ Jy km s}^{-1}$ (J1553+3548) and $\int S dV < 0.069 \times (\Delta V/100)^{1/2} \text{ Jy km s}^{-1}$ (J1619+3342) on the integrated H I 21cm line flux density, and $M_{\text{HI}} < 2.3 \times 10^9 \times (\Delta V/100)^{1/2} M_{\odot}$ (J1553+3548) and $M_{\text{HI}} < 2.7 \times 10^9 \times (\Delta V/100)^{1/2} M_{\odot}$ (J1619+3342) on the H I masses of the two absorbers.

Table 1 summarizes our current knowledge of the atomic gas

masses of low- z DLAs and sub-DLAs. The sample consists of five systems, two DLAs and three sub-DLAs. H I 21cm emission has been detected in only two objects, the $z \approx 0.0063$ sub-DLA towards PG 1216+069 (Briggs & Barnes 2006) and the $z \approx 0.009$ DLA towards SBS 1549+543 (Bowen et al. 2001). Table 1 also lists the H I column densities of the absorbers and (when available) their metallicities and velocity widths.

It is clear from Table 1 that the inferred H I masses or limits on the H I mass are in all cases significantly lower (by a factor of at least a few) than the H I mass at the knee of the Schechter function that provides a good fit to the H I mass distribution of galaxies in the local Universe, $\log[M_{\text{HI}}^*/M_{\odot}] = (9.96 \pm 0.02)$ (Martin et al. 2010), us-

Table 1. Summary of searches for H I 21cm emission in DLAs and sub-DLAs.

QSO	z_{DLA}	N_{HI} $\times 10^{20} \text{ cm}^{-2}$	M_{HI}^a M_{\odot}	$[Z/H]^b$	Reference
PG 1216+069	0.0063	0.2	1.5×10^7	-1.60 ± 0.10	1,2,11
SBS 1543+543	0.009	2.2	1.3×10^9	-0.41 ± 0.06	3,4,5
SDSS J1553+3548	0.0830	0.35	$< 2.3 \times 10^9$	-1.10 ± 0.16	6,7,8
SDSS J1619+3342	0.0963	3.5	$< 2.7 \times 10^9$	-0.62 ± 0.13	6,7,8
PKS 0439–433	0.101	0.71	$< 3.7 \times 10^9$	-0.42 ± 0.12	9,10

(1) Kanekar & Chengalur 2005; (2) Briggs & Barnes 2006; (3) Bowen et al. 2001; (4) Chengalur & Kanekar 2002; (5) Bowen et al. 2005; (6) Meiring et al. 2011; (7) this work; (8) Battisti et al. 2012; (9) Kanekar et al. 2001; (10) Chen et al. 2005; (11) Tripp et al. 2005.

^a The H I masses have been scaled to the Λ CDM cosmology used in this paper, with 3σ mass limits quoted at a velocity resolution of 100 km s^{-1} .

^b The quoted metallicities $[Z/H]$ are based on $[O/H]$ (PG1216+069; Tripp et al. 2005), $[S/H]$ (SBS1543+593 and SDSS J1619+3342; Bowen et al. 2005), $[Si/H]$ (SDSS J1553+3548; Battisti et al. 2012) and $[Fe/H]+0.3$ (PKS 0439–433; Chen et al. 2005; Rafelski et al. 2012).

ing $H_0 = 67.3 \text{ km s}^{-1} \text{ Mpc}^{-1}$. Thus, although the number of damped systems that have so far been searched for H I 21cm emission is still quite small, the present data indicate that low-redshift DLAs and sub-DLAs do not typically arise in massive, gas-rich galaxies.

It is interesting to compare our results with the predictions of Zwaan et al. (2005) for the typical H I mass of low- z DLAs. Zwaan et al. (2005) used Westerbork Synthesis Radio Telescope H I 21cm emission images of a large sample of nearby galaxies to test whether high- z DLAs might arise in galaxies with gas distributions similar to that in the $z = 0$ galaxy population. They found both the incidence rate, and the distribution of impact parameters and H I column densities, of low- z DLAs to be consistent with a scenario in which the absorbers arise in the local galaxy population. The median $z = 0$ DLA is expected to arise in a low-luminosity ($L^*/7$) galaxy, with an H I mass of $2 \times 10^9 M_{\odot}$. While high-mass DLAs do contribute significantly to the cross-section, it is the highest H I column densities that tend to arise in the most massive galaxies. Comparing with our results, it is clear from Table 1 that the five DLAs and sub-DLAs at $z \lesssim 0.1$ that have so far been searched for H I 21cm emission all have low N_{HI} values, $\leq 3.5 \times 10^{20} \text{ cm}^{-2}$, and low H I masses, $< 3.7 \times 10^9 M_{\odot}$. Our results are thus entirely consistent with the predictions of Zwaan et al. (2005). It would be interesting to search for H I 21cm emission from low- z DLAs with high H I column densities, for which Zwaan et al. (2005) expect the cross-section to be dominated by massive galaxies.

There have been suggestions in the literature that sub-DLAs (also known as super-Lyman limit systems, with $10^{19} \text{ cm}^{-2} \leq N_{\text{HI}} \leq 2 \times 10^{20} \text{ cm}^{-2}$) arise in galaxies that are systematically more massive than the galaxies that give rise to DLAs (e.g. Khare et al. 2007; Kulkarni et al. 2010, but see Dessauges-Zavadsky et al. 2009). We emphasize that the three sub-DLAs of Table 1 also have low H I masses, $< 3.7 \times 10^9 M_{\odot}$, contradicting the above arguments. Of course, our conclusion is tempered by sample variance and must be tested with a much larger survey.

Finally, the metallicity of DLAs is known to show a correlation with the velocity width V_{90} of unsaturated low-ionization metal lines (Wolfe & Prochaska 1998; Ledoux et al. 2006), as well as with the rest equivalent width of saturated metal lines (Prochaska et al. 2008). These correlations have usually been interpreted in terms of a mass-metallicity relation in the absorbers (e.g. Ledoux et al. 2006; Møller et al. 2013; Neeleman et al. 2013), similar to the mass-metallicity relation that has been found in high- z emission-selected galaxies (e.g. Tremonti et al. 2004; Erb et al.

2006; Maiolino & et al. 2008). Three of the absorbers of Table 1 have high metallicities, $[Z/H] \geq -0.62$, in the top 10% of DLA metallicities at all redshifts (e.g. Rafelski et al. 2012). It is interesting that all three of these high-metallicity absorbers show low H I masses, $M_{\text{HI}} < 3.7 \times 10^9 M_{\odot}$. We thus find that absorbers with high metallicities do not necessarily have high gas masses, in apparent contradiction with the putative mass-metallicity relation. However, it should be emphasized that the metallicity estimates only probe a pencil beam through the three galaxies; testing the mass-metallicity relation would require a larger sample. Further, the mass-metallicity relation for emission-selected galaxies involves the *stellar* mass while that for DLAs involves the *virial* mass (dominated by dark matter), neither of which can be immediately linked to the gas mass.

In summary, we have carried out a deep GBT search for redshifted H I 21cm emission from three DLAs and sub-DLAs at $z \approx 0.1$. Our GBT non-detections of H I 21cm emission yield tight constraints on the H I mass of two absorbers, $M_{\text{HI}} < 2.3 \times 10^9 \times (\Delta V/100)^{1/2} M_{\odot}$ for the $z = 0.0830$ sub-DLA towards J1553+3548, and $M_{\text{HI}} < 2.7 \times 10^9 \times (\Delta V/100)^{1/2} M_{\odot}$ for the $z = 0.0963$ DLA towards J1619+3342. The data on the third absorber, at $z = 0.114$ towards J1009+0713, was rendered unusable by strong RFI close to the redshifted H I 21cm line frequency. Our results are consistent with a scenario in which most low-H I column density DLAs and sub-DLAs at low redshifts do not arise in massive gas-rich galaxies.

ACKNOWLEDGEMENTS

PM acknowledges support from the NCRA-TIFR Visiting Students' Research Programme, and NK from the Department of Science and Technology through a Ramanujan Fellowship. JXP is partly supported by NSF grant AST-1109447. The NRAO is a facility of the National Science Foundation operated under cooperative agreement by Associated Universities, Inc.. We thank an anonymous referee for a careful reading of an earlier version of this paper.

REFERENCES

Battisti A. J., Meiring J. D., Tripp T. M., Prochaska J. X., Werk J. K., Jenkins E. B., Lehner N., Tumlinson J., Thom C., 2012,

- ApJ, 744, 93
- Bowen D. V., Huchtmeier W., Brinks E., Tripp T. M., Jenkins E. B., 2001, A&A, 372, 820
- Bowen D. V., Jenkins E. B., Pettini M., Tripp T. M., 2005, ApJ, 635, 880
- Briggs F. H., Barnes D. G., 2006, ApJ, 640, L127
- Chen H.-W., Kennicutt Jr. R. C., Rauch M., 2005, ApJ, 620, 703
- Chengalur J. N., Kanekar N., 2002, A&A, 388, 383
- Dessauges-Zavadsky M., Ellison S. L., Murphy M. T., 2009, MNRAS, 396, L61
- Dessauges-Zavadsky M., Prochaska J. X., D’Odorico S., Calura F., Matteucci F., 2006, A&A, 445, 93
- Erb D. K., Shapley A. E., Pettini M., Steidel C. C., Reddy N. A., Adelberger K. L., 2006, ApJ, 644, 813
- Fumagalli M., O’Meara J. M., Prochaska J. X., Kanekar N., 2010, MNRAS, 408, 362
- Haehnelt M. G., Steinmetz M., Rauch M., 1998, ApJ, 495, 64
- Kanekar N., Chengalur J. N., 2001, A&A, 369, 42
- Kanekar N., Chengalur J. N., 2003, A&A, 399, 857
- Kanekar N., Chengalur J. N., 2005, A&A, 429, L51
- Kanekar N., Chengalur J. N., Subrahmanyan R., Petitjean P., 2001, A&A, 367, 46
- Kanekar N., Prochaska J. X., Smette A., Ellison S. L., Ryan-Weber E. V., Momjian E., Briggs F. H., Lane W. M., Chengalur J. N., Delafosse T., Grave J., Jacobsen D., de Bruyn A. G., 2014, MNRAS, 438, 2131
- Kanekar N., Smette A., Briggs F. H., Chengalur J. N., 2009, ApJ, 705, L40
- Kanekar N., Subrahmanyan R., Ellison S. L., Lane W. M., Chengalur J. N., 2006, MNRAS, 370, L46
- Khare P., Kulkarni V. P., Péroux C., York D. G., Lauroesch J. T., Meiring J. D., 2007, A&A, 464, 487
- Krogager J.-K., Fynbo J. P. U., Møller P., Ledoux C., Noterdaeme P., Christensen L., Milvang-Jensen B., Sparre M., 2012, MNRAS, 424, L1
- Kulkarni V. P., Khare P., Som D., Meiring J., York D. G., Péroux C., Lauroesch J. T., 2010, New Astronomy, 15, 735
- le Brun V., Bergeron J., Boissé P., Deharveng J.-M., 1997, A&A, 321, 733
- Ledoux C., Petitjean P., Fynbo J. P. U., Møller P., Srianand R., 2006, A&A, 457, 71
- Ledoux C., Petitjean P., Srianand R., 2003, MNRAS, 346, 209
- Maiolino R., et al. 2008, A&A, 488, 463
- Martin A. M., Papastergis E., Giovanelli R., Haynes M. P., Springob C. M., Stierwalt S., 2010, ApJ, 723, 1359
- Meiring J. D., Tripp T. M., Prochaska J. X., Tumlinson J., Werk J., Jenkins E. B., Thom C., O’Meara J. M., Sembach K. R., 2011, ApJ, 732, 35
- Møller P., Fynbo J. P. U., Ledoux C., Nilsson K. K., 2013, MNRAS, 430, 2680
- Neeleman M., Wolfe A. M., Prochaska J. X., Rafelski M., 2013, ApJ, 769, 54
- Noterdaeme P., Ledoux C., Petitjean P., Srianand R., 2008, A&A, 481, 327
- Noterdaeme P., Petitjean P., Ledoux C., Srianand R., 2009, A&A, 505, 1087
- O’Meara J. M., Prochaska J. X., Burles S., Prochter G., Bernstein R. A., Burgess K. M., 2007, ApJ, 656, 666
- Péroux C., Bouché N., Kulkarni V. P., York D. G., Vladilo G., 2012, MNRAS, 419, 3060
- Planck Collaboration 2013, arxiv:1303.5076
- Prochaska J. X., Chen H.-W., Wolfe A. M., Dessauges-Zavadsky M., Bloom J. S., 2008, ApJ, 672, 59
- Prochaska J. X., Gawiser E., Wolfe A. M., Castro S., Djorgovski S. G., 2003, ApJ, 595, L9
- Prochaska J. X., Herbert-Fort S., Wolfe A. M., 2005, ApJ, 635, 123
- Prochaska J. X., Wolfe A. M., 1997, ApJ, 487, 73
- Rafelski M., Wolfe A. M., Prochaska J. X., Neeleman M., Mendez A. J., 2012, ApJ, 755, 89
- Rao S. M., Nestor D. B., Turnshek D. A., Lane W. M., Monier E. M., Bergeron J., 2003, ApJ, 595, 94
- Rohlfs K., Wilson T. L., 2006, Tools of Radio Astronomy, 4th ed.. Berlin: Springer
- Tremonti C. A., Heckman T. M., Kauffmann G., Brinchmann J., Charlot S., White S. D. M., Seibert M., Peng E. W., Schlegel D. J., Uomoto A., Fukugita M., Brinkmann J., 2004, ApJ, 613, 898
- Tripp T. M., Jenkins E. B., Bowen D. V., Prochaska J. X., Aracil B., Ganguly R., 2005, ApJ, 619, 714
- Tumlinson J., Thom C., Werk J. K., Prochaska J. X., Tripp T. M., Katz N., Davé R., Oppenheimer B. D., Meiring J. D., Ford A. B., O’Meara J. M., Peebles M. S., Sembach K. R., Weinberg D. H., 2013, ApJ, 777, 59
- Wiklund T., Combes F., 1994, A&A, 286, L9
- Wolfe A. M., Prochaska J. X., 1998, ApJ, 494, L15
- Zwaan M. A., van der Hulst J. M., Briggs F. H., Verheijen M. A. W., Ryan-Weber E. V., 2005, MNRAS, 364, 1467